Article

Cell Reports

SEEDSTICK Controls *Arabidopsis* Fruit Size by Regulating Cytokinin Levels and *FRUITFULL*

Graphical Abstract

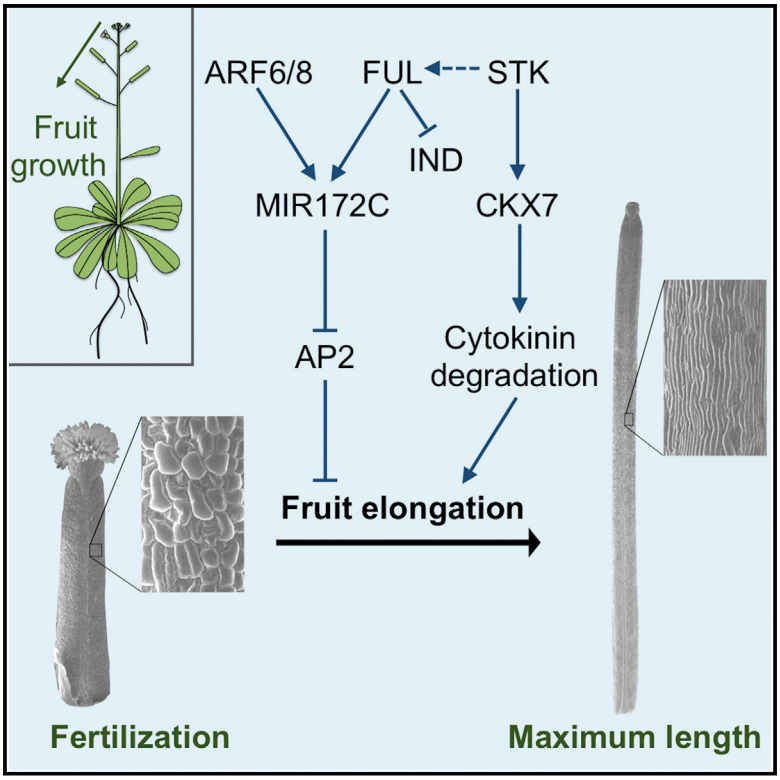

Highlights

- Modulation of the cytokinin pathway is critical for determining fruit size
- Cytokinins play opposing roles in pistil/fruit growth before and after fertilization
- SEEDSTICK integrates cytokinin and molecular pathways to regulate fruit size

Authors

Maurizio Di Marzo, Humberto Herrera-Ubaldo, Elisabetta Caporali, ..., Marta A. Mendes, Stefan de Folter, Lucia Colombo

Correspondence

lucia.colombo@unimi.it

In Brief

Di Marzo et al. establish that defects in *Arabidopsis* fruit size are accompanied by alterations in the metabolism of the plant hormone cytokinin, which is critical for cell elongation. SEEDSTICK influences fruit elongation by directly regulating cytokinin degradation via CKX7 and indirectly modulating the expression of the MADS-box gene *FRUITFULL*.

Di Marzo et al., 2020, Cell Reports *30*, 2846–2857
February 25, 2020
https://doi.org/10.1016/j.celrep.2020.01.101

CellPress

OPEN ACCESS
CellPress

Cell Reports
Article

SEEDSTICK Controls *Arabidopsis* Fruit Size by Regulating Cytokinin Levels and *FRUITFULL*

Maurizio Di Marzo,[1] Humberto Herrera-Ubaldo,[2] Elisabetta Caporali,[1] Ondřej Novák,[3] Miroslav Strnad,[3] Vicente Balanzà,[1,4] Ignacio Ezquer,[1] Marta A. Mendes,[1] Stefan de Folter,[2] and Lucia Colombo[1,5,*]

[1]Dipartimento di BioScienze, Università degli Studi di Milano, Milan, Milan 20133, Italy
[2]Unidad de Genómica Avanzada (LANGEBIO), Centro de Investigación y de Estudios Avanzados del Instituto Politécnico Nacional (CINVESTAV-IPN), Irapuato, Guanajuato 36824, México
[3]Laboratory of Growth Regulators, Faculty of Science of Palacký University & Institute of Experimental Botany of the Czech Academy of Sciences, Olomouc, Olomouc 78371, Czech Republic
[4]Instituto de Biologia Molecular y Celular de Plantas, Consejo Superior de Investigacione Cientificas, Universidad Politecnica de Valencia, Valencia, Valencia 46022, Spain
[5]Lead Contact
*Correspondence: lucia.colombo@unimi.it
https://doi.org/10.1016/j.celrep.2020.01.101

SUMMARY

Upon fertilization, the ovary increases in size and undergoes a complex developmental process to become a fruit. We show that cytokinins (CKs), which are required to determine ovary size before fertilization, have to be degraded to facilitate fruit growth. The expression of *CKX7*, which encodes a cytosolic CK-degrading enzyme, is directly positively regulated post-fertilization by the MADS-box transcription factor STK. Similar to *stk*, two *ckx7* mutants possess shorter fruits than wild type. Quantification of CKs reveals that *stk* and *ckx7* mutants have high CK levels, which negatively control cell expansion during fruit development, compromising fruit growth. Overexpression of *CKX7* partially complements the *stk* fruit phenotype, confirming a role for CK degradation in fruit development. Finally, we show that STK is required for the expression of *FUL*, which is essential for valve elongation. Overall, we provide insights into the link between CKs and molecular pathways that control fruit growth.

INTRODUCTION

Fruit, whose main function is to protect and disperse its seeds, has contributed to the evolutionary success of angiosperms. The dry and dehiscent fruit of *Arabidopsis* is a silique formed by two lateral valves and separated from the central replum by the valve margin tissue. The differentiation and development of the fruit from the ovary is triggered by the double-fertilization process (stage 13), and the fruit reaches its maximum length at stage 17-B (Ferrándiz et al., 1999; Roeder and Yanofsky, 2006). Double fertilization causes a local increase in auxin concentration, which results in the activation of gibberellin (GA) biosynthesis. The synchronized action of the two hormones controls the differentiation of the ovary into a fruit (Alabadí et al., 2009). AUXIN RESPONSE FACTOR (ARF) 6 and ARF8 interact with the MADS-box transcription factor FRUITFULL (FUL) to recruit microRNA 172c (miR172c), which is required to inhibit the repressor of fruit elongation, *APETALA 2* (*AP2*) (José Ripoll et al., 2015). FUL also represses the expression of *INDEHISCENT* (*IND*), which encodes a basic-helix-loop-helix (bHLH) transcription factor that negatively regulates fruit growth (Liljegren et al., 2004).

Cytokinins (CKs) have been implicated in regulating placenta length/size and determining ovule number (Cucinotta et al., 2016). Indeed, higher-order *crf* (*cytokinin response factor*) mutants possess fewer ovules and smaller placentas, which suggests they have defects in cell proliferation and/or expansion (Cucinotta et al., 2016).

CKs are also involved in valve margin differentiation (Marsch-Martínez et al., 2012). The *IND* fruit phenotype of *shp1 shp2* double mutants, which results from defects in valve margin differentiation (Liljegren et al., 2000), can be rescued by exogenous CK treatment (Marsch-Martínez et al., 2012). The CYTOKININ OXIDASE/DEHYDROGENASE (CKX) proteins catalyze the irreversible inactivation of CKs, transforming them to adenine and a corresponding side chain-derived aldehyde (Mok and Mok, 2001; Spíchal, 2012). The CKX enzymes differ in their subcellular localization, chemical characteristics, and substrate specificity (Galuszka et al., 2007; Werner et al., 2003). Reduced CK degradation in the *ckx3 ckx5* double mutant causes an increase in pistil length and a consequent increase in seed yield (Bartrina et al., 2011). The *CKX7* gene is one of the seven members of the CKX family (Mok and Mok, 2001). It encodes a unique CKX protein that localizes to the cytosolic compartment of the cell, where it degrades a specific CK pool (Köllmer et al., 2014). The CKX7 protein has the lowest similarity to other *Arabidopsis* CKX members but is more similar to CKX-like proteins of bacteria and green algae (Schmülling et al., 2003). It has been reported that CKX7 is required for appropriate root growth and xylem differentiation (Köllmer et al., 2014).

In this manuscript, we report the function of CKX7 and CKs in fruit elongation and the role of the MADS-box transcription factor SEEDSTICK (STK) as a central integrator of the CK hormonal pathway and the molecular network controlling fruit size.

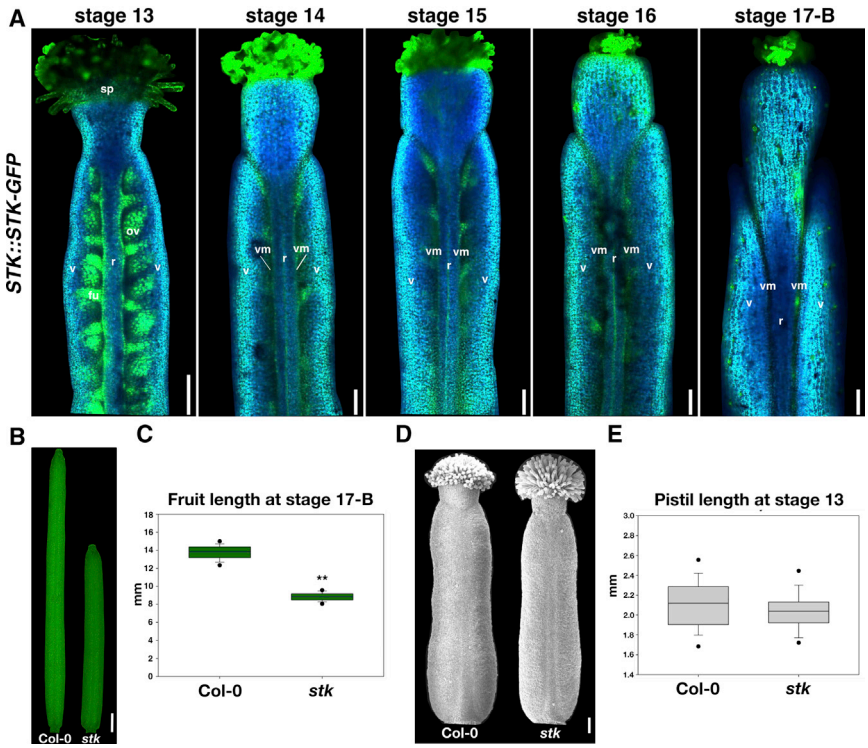

Figure 1. STK Protein Localization and Morphological Characterization of *stk* Fruit and Pistils

(A) Confocal images of *STK::STK-GFP* (Col-0) in pistils (stage 13) and during fruit elongation stages (stages 14 to 17-B). r, replum; sp, stigma papillae; v, valve; vm, valve margin. Scale bars, 100 μm.

(B) Stereomicroscope images of *stk* and Col-0 siliques at stage 17-B. Scale bar, 1 mm.

(C) Boxplot representing *stk* and Col-0 silique length at stage 17-B. Boxes indicate the first quartile (Q1), the mean, and the third quartile (Q3); the black dots represent maximum and minimum values. The length of the fruits was evaluated by measuring 20 siliques for each genotype for three biological replicates. Statistical analysis was performed using Student's t test (**$p < 0.01$).

(D) SEM imaging of *stk* and Col-0 pistils at stage 13. Scale bar, 100 μm.

(E) Boxplot representing *stk* and Col-0 pistil length at stage 13. Boxes indicate the first quartile (Q1), the mean, and the third quartile (Q3); the black dots represent maximum and minimum values. The length of the pistils was evaluated by measuring 20 pistils for each genotype in two biological replicates.

RESULTS

STK Is Required for Fruit Elongation

Recently, the presence of *STK* transcripts has been demonstrated in siliques at different developmental stages (Mizzotti et al., 2018). To better characterize the localization of the STK protein, we analyzed the *STK::STK-GFP* (Mizzotti et al., 2014) marker line in pistils during anthesis (stage 13) and in siliques from stage 14 to stage 17-B. During fertilization (stage 13), the STK-GFP protein was localized to stigma papillae, the funiculus, ovules, and the replum (Figure 1A). During fruit growth, the protein was localized within the medial domain of the fruit, in the vascular bundle of the replum, and in the valve margin from stage 14 to stage 16 (Figure 1A). At stage 17-B, no GFP signal was observed in the replum, whereas it was still detected in the valve margin (Figure 1A).

The *stk* mutant is characterized by shorter fruits than wild type (Pinyopich et al., 2003; Herrera-Ubaldo et al., 2019). At stage 17-B, when siliques reach their maximum size and length (Ferrándiz et al., 1999; Roeder and Yanofsky, 2006), the *stk* mutant is characterized by shorter fruits than those of wild type (*stk*: mean = 8.84 mm, n = 60; Col-0: mean = 13.82 mm, n = 60) (Figures 1B and 1C). However, the length of *stk* pistils (Figures 1D and 1E) at anthesis did not differ significantly from that of wild-type pistils (*stk*: mean = 2.03 mm, n = 40; Col-0: mean = 2.11, n = 40). These data show that STK positively regulates fruit elongation following fertilization.

CK Signaling Is Altered in *stk* during Fruit Elongation

CKs positively regulate pistil development, and a deficiency in CK production, perception, or response causes a decrease in pistil size (Cucinotta et al., 2016, 2018; Reyes-Olalde et al., 2017). By contrast, an increase in the amount of CKs and consequently CK response causes an increase in pistil size (Bartrina et al., 2011). However, the role of CKs in determining silique length has not previously been described. Therefore, we studied CK signaling in *stk* pistils and fruits with respect to the wild type, using the *TCSn::GFP* marker that is activated in response to CKs (Zürcher et al., 2013). The GFP signal was localized to the medial domain, the replum, and the style and stigma of wild-type pistils before fertilization at stage 12 (Figure 2A). A similar pattern of GFP expression was detected in *stk* (Figure 2G). At stage 13, there was a clear increase in GFP signal in the replum and style of *stk* with respect to wild type (Figures 2B and 2H). During fruit elongation, CK signaling decreased in the medial domain of wild-type fruit. In particular, a weak GFP signal was still detected in the replum at stage 14 (Figure 2C), whereas from stage 15 onward, no GFP was visible (Figures 2D–2F). By contrast, *TCSn* was still active in the *stk* replum and style at stage 14 (Figure 2I), in the replum at stage 15 (Figure 2J), and in the valve margin at stage 16 (Figure 2K), whereas no GFP was detected at stage 17-B (Figure 2L). In conclusion, wild-type CK signaling decreased after fertilization, concomitant with the onset of fruit elongation, whereas in *stk*, CK signaling remained detectable until at least stage 16.

STK Directly Regulates *CKX7* Expression

To understand the basis for the increased CK signaling in *stk* mutant fruit with respect to wild type (Figure 2), we hypothesized that a difference might exist in the activity of the genes involved in CK metabolism. We particularly focused on CK

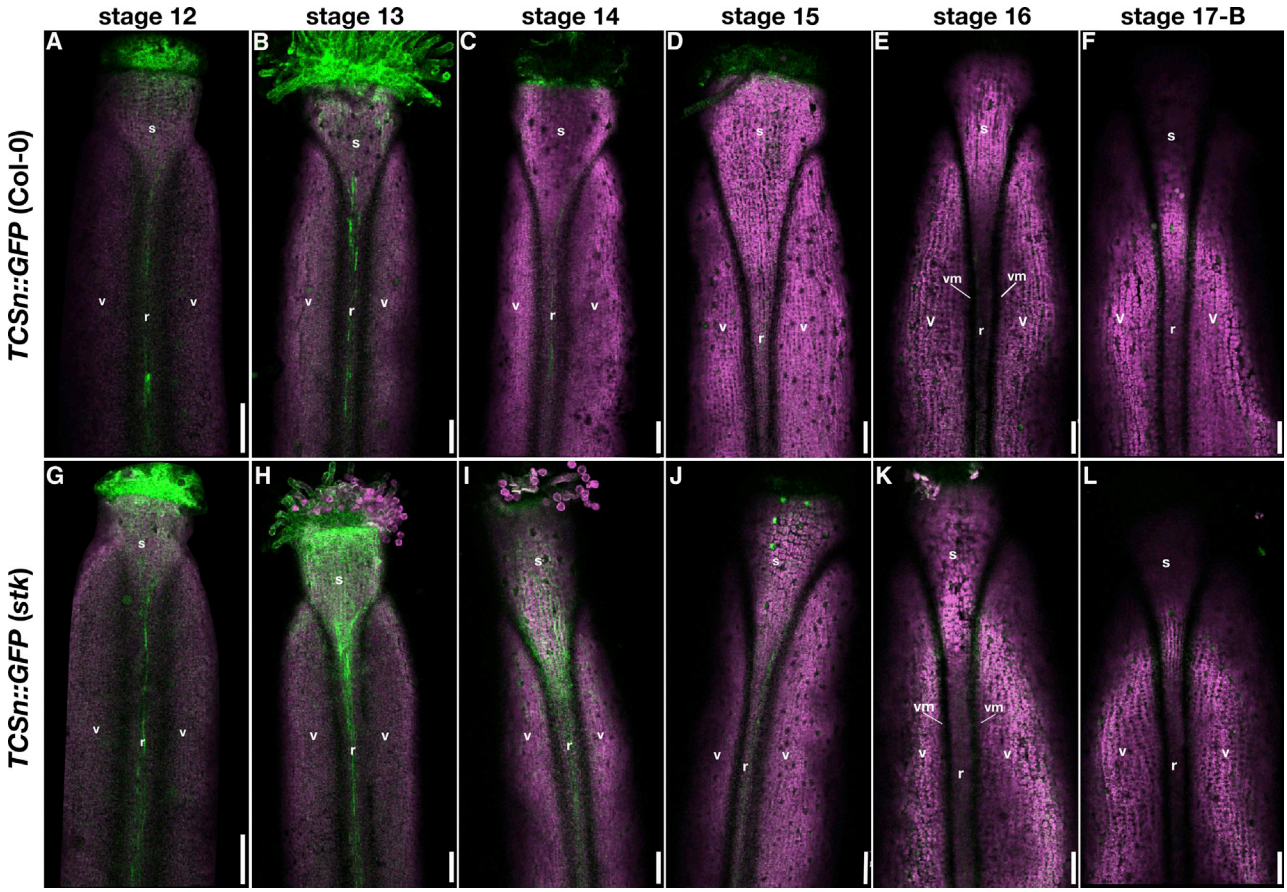

Figure 2. Comparative *In Vivo* CK Signaling in Pistils and Fruits of *stk* and Col-0, Revealed by Confocal Imaging Using the *TCSn::GFP* Marker

(A–F) *TCSn::GFP* expression in Col-0. Stage 12 pistil before fertilization (A), stage 13 pistil during fertilization (B), stage 14 of fruit development (C), stage 15 of fruit development (D), stage 16 of fruit development (E), and stage 17-B of fruit development (F).

(G–L) *TCSn::GFP* expression in *stk*. Stage 12 pistil (G), stage 13 (H), stage 1 (I) 4, stage 15 (J), stage 16 (K), and stage 17-B (L). r, replum; s, style; v, valve; vm, valve margin. Scale bars, 100 μm.

degradation, which is catalyzed by the CKX enzymes that regulate the amount of CKs in cells (Mok and Mok, 2001; Spíchal, 2012). We performed qPCR to quantify expression of the *CKX* genes in wild-type and *stk* mutant pistils/siliques at stages 13–14, 15–16, 17-A, and 17-B of fruit growth. We analyzed the transcript levels of *CKX1*, *CKX3*, and *CKX5*, whose roles in pistil/silique development have been previously described (Bartrina et al., 2011; Werner et al., 2003), as well as that of *CKX6*, whose promoter is active in the funiculus (Werner et al., 2003), and *CKX7*, which is expressed in fruits of different species, including *Arabidopsis thaliana*, *Brassica napus*, and *Malus domestica* (Liu et al., 2018; Mizzotti et al., 2018; Tan et al., 2018). The comparative analysis of *CKX* expression revealed that only *CKX7* expression was lower in *stk* than in wild type at stages 13–14, 15–16, 17-A, and 17-B (Figure 3A). We analyzed *CKX7* promoter activity in *stk* at the same stages used for expression analysis, using the *pCKX7::GUS* construct. The *CKX7* promoter was active in the vascular tissues of the pistil and fruit (Figure 3B; see also Figure S1). In wild type, the **β-glucuronidase** (GUS) signal was present in the lateral vascular bundles of the valves and in the vascular bundle of the replum following fertilization and during fruit elongation (up to stage 17-B) (Figure 3B). However, no *CKX7* promoter activity was observed in *stk* at all stages analyzed (Figure 3B). These results suggest that STK might control CK degradation by transcriptionally regulating *CKX7*. To determine whether STK directly regulates *CKX7*, we performed a chromatin immunoprecipitation (ChIP) assay using anti-GFP antibodies and chromatin from *stk* siliques up to stage 16, from plants expressing *STK::STK-GFP* (Mizzotti et al., 2014). We analyzed the *CKX7* promoter sequence for the presence of MADS-domain CArG-box binding sites (Egea-Cortines et al., 1999; de Folter and Angenent, 2006). Among the eight putative CArG boxes we identified in the *CKX7* promoter and tested for direct binding by STK, the ChIP assay revealed significant enrichment of binding to the regions spanning CArG-box 4 and CArG-box 5 in the *CKX7* promoter in *STK::STK-GFP* compared with the wild-type control (Figure 3C). Therefore, STK can directly bind the *CKX7* promoter, and the increased level of CK signaling observed in *stk* medial fruit tissues during fruit elongation might result from a local downregulation of *CKX7*, which is responsible for cytosolic CK degradation in cells in these tissues.

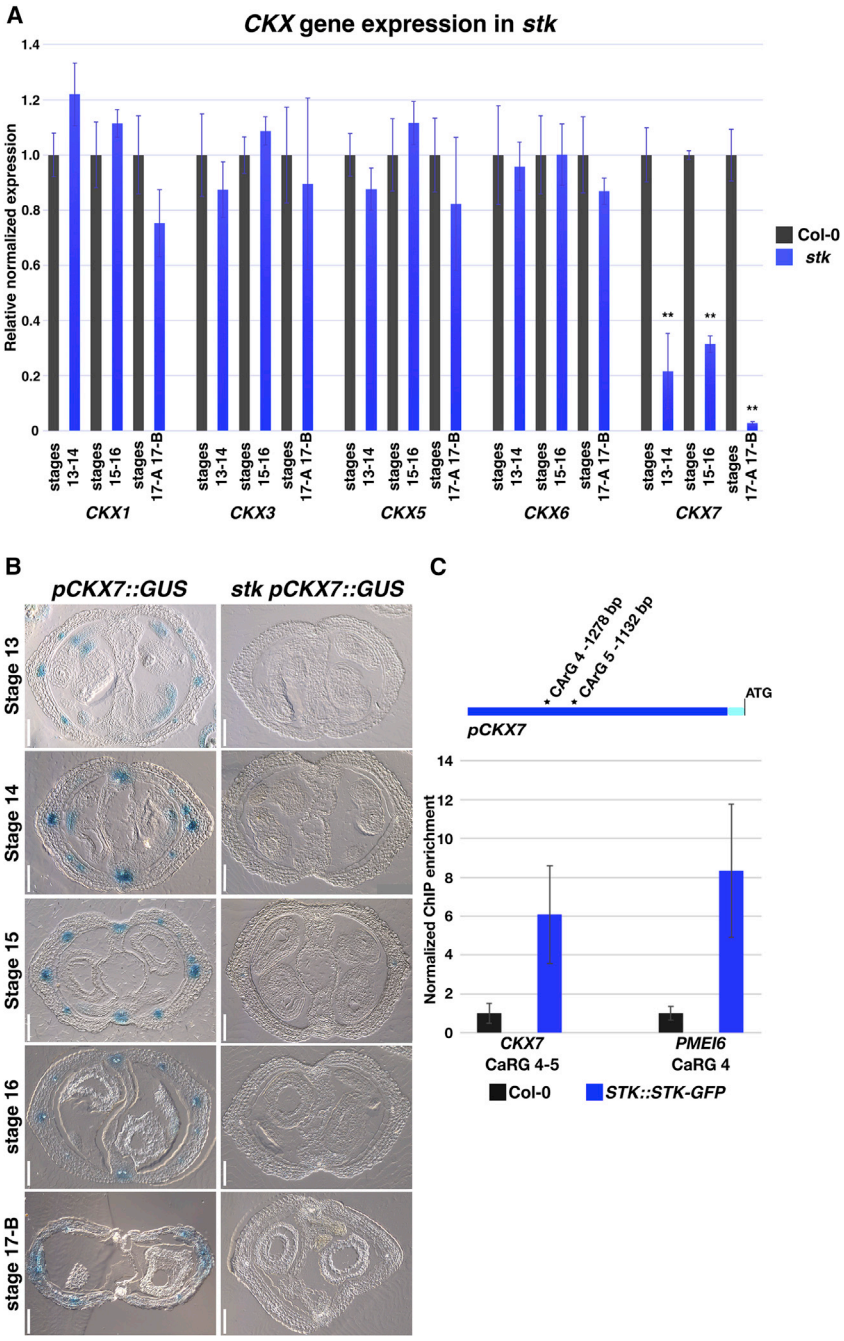

Figure 3. STK Directly Regulates *CKX7* Expression

(A) Expression of *CKX1*, *CKX3*, *CKX5*, *CKX6*, and *CKX7* in *stk* and Col-0 at stages 13–14, 15–16, 17-A, and 17-B. Statistical analysis was performed using Student's t test (**$p < 0.01$) and gene expression was normalized to that of *ACTIN* and *UBIQUITIN*. Histograms show a representative experiment in which error bars represent the SD for three technical replicates. Three qPCR (biological replicates) were performed and generated similar results.

(B) Cross-sections showing expression of *pCKX7::GUS* from stage 13 to stage 17-B in *stk* and Col-0. Scale bars, 100 μm. At the right bottom corner of the stk pCKX7::GUS (stage 14) image the scale bar automatically generated by the microscope has been covered to show uniform scale bars in this panel.

(C) Representation of the *CKX7* promoter showing the position of the CArG boxes. Representative ChIP experiment between *STK::STK-GFP* and Col-0. Error bars represent the SD for three technical replicates. The fold enrichment was calculated against data for Col-0. *PECTIN METHYLESTERASE INHIBITOR 6* (*PMEI6*) CArG 4 was used as a positive, and data were normalized with *ACTIN2/7*.

The CK Cytosolic Pool Regulates Cell Elongation during Fruit Development

To evaluate the role of *CKX7* during fruit elongation, we investigated the phenotype of two independent *ckx7* mutants and a *35S::CKX7* overexpression line. The first *ckx7* mutant allele contained a transfer DNA (T-DNA) insertion in the second intron (*ckx7* SAIL_515_A07). We generated a second mutant allele using CRISPR/Cas9 technology. The second mutant allele (named *ckx7 T*) carried a T insertion within the first exon at position 254 from the ATG start (Figure S2A). This insertion causes a frameshift in the FAD binding domain and the formation of a premature stop codon after 129 aa, creating a truncated protein with no enzymatic activity (Bae et al., 2008). The pistils of stage 13 *ckx7*, *ckx7 T*, and *35S::CKX7* plants were the same length as wild-type pistils (Figures S3A and S3B). At stage 17-B, the fruits of *ckx7* and *ckx7 T* plants were shorter (*ckx7* = 10.87 mm, n = 60; *ckx7 T* = 12.45 mm, n = 60) than those of wild type (Col-0 = 13.54 mm, n = 60) but were longer than those of *stk* (Figures 4A and 4B, see also Figures 1B and 1C). Conversely, the overexpression line *35S::CKX7* produced longer fruits (*35S::CKX7* = 15.13 mm, n = 60) than wild-type plants (Figures 4A and 4B). Altogether, the data suggest a positive role for *CKX7* in promoting fruit elongation following fertilization.

To clarify the potential role of CKs in cell proliferation and/or elongation during fruit maturation, we analyzed in detail the shape and morphology of the valve cells in *stk*, *ckx7*, and *ckx7 T* and the overexpression line *35S::CKX7* at stage 17-B (Figures 4C–4H). We analyzed valve cells, because it has been demonstrated that increased fruit size results from the elongation of epidermal cells (Vivian-Smith et al., 2001). We used Feulgen staining, adapted for siliques, to analyze cell morphology (Braselton et al., 1996). The total number of valve cells in *stk*, *ckx7*, and *ckx7 T* mutants and in the *35S::CKX7* overexpression line was similar to that of wild type, whereas cell length differed among the various genotypes (Figures 4C–4H). Specifically, mean cell length in *stk* valves (Figure 4D) was lower

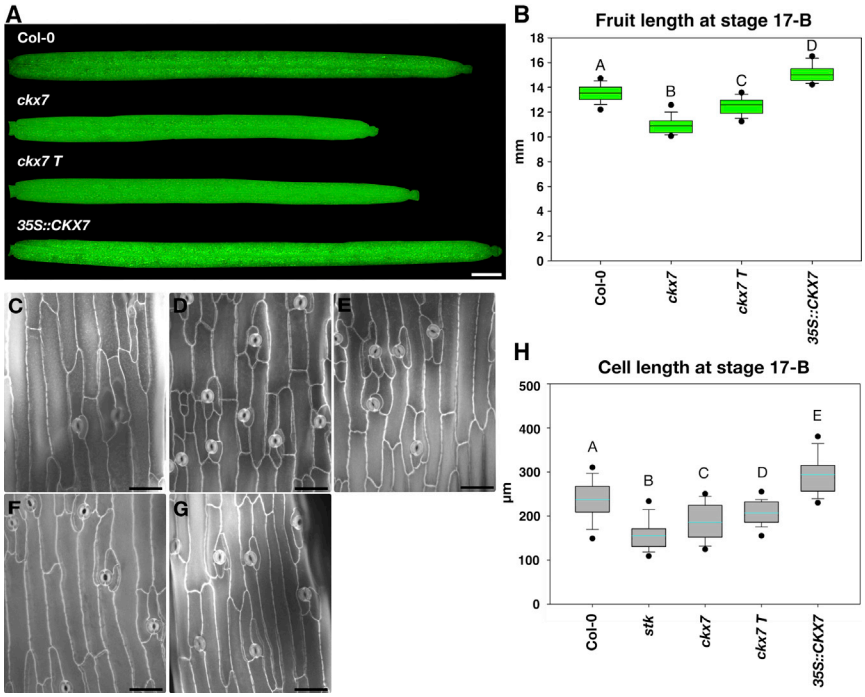

Figure 4. CK Degradation Is Essential for Correct Fruit Elongation

(A) Stereomicroscope images of *ckx7*, *ckx7 T*, *35S::CKX7*, and Col-0 siliques at stage 17-B. Scale bar, 1 mm.

(B) Boxplot representing the fruit length for the genotypes in (A). Boxes indicate the first quartile (Q1), the mean, and the third quartile (Q3); the black dots represent maximum and minimum values. The length of the fruits was evaluated by measuring 20 siliques for each genotype for three biological replicates.

(C–G) Confocal images of valve fruit cells: (C) Col-0, (D) *stk*, (E) *ckx7*, (F) *ckx7 T*, and (G) *35S::CKX7*. Scale bars, 50 μm.

(H) Boxplot representing cell length in the mutants and the overexpression line. Boxes indicate the first quartile (Q1), the mean, and the third quartile (Q3); the black dots represent maximum and minimum values. Cell length was evaluated by measuring 30 cells for each genotype for three biological replicates.

Statistical analyses were performed using ANOVA followed by Tukey's HSD test. Different letters indicate statistically significant differences ($p < 0.01$).

than in wild type (Figure 4C) (*stk* = 155.11 μm, Col-0 = 237.33 μm, Figure 4H). A similar decrease in cell length was observed for the two *ckx7* mutant alleles (Figures 4E and 4F) (*ckx7* = 185.38 μm, *ckx7 T* = 206.82 μm, Figure 4H), whereas valve cells in *35S::CKX7* plants (Figure 4G) were longer than cells in wild type (*35S::CKX7* = 281.26 μm, Figure 4H).

In conclusion, the valve cells of *stk*, *ckx7*, and *ckx7 T* mutants, from which the absence of CKX7 causes an increase in the pool of cytosolic CKs, were shorter than in wild type; conversely, those in the *35S::CKX7* line were longer. These data suggest that the cytosolic CK pool plays an important role in the regulation of cell elongation and consequently in the regulation of fruit growth.

The Quantity of *cis*-Zeatin (*c*Z) and *trans*-Zeatin (*t*Z) CKs in *stk*, *ckx7*, and *ckx7 T* Is Affected during Fruit Growth

To evaluate whether the increased and more persistent activity of the *TCSn* marker in *stk* (Figure 2) resulted from an increase in CK concentration in developing siliques, we performed a metabolic analysis in which we quantified CKs. In particular, we quantified CKs at early stages of fruit growth (from stage 13 to stage 16) and at late stages of fruit elongation (stages 17-A and 17-B) in *stk* and in the two single mutants *ckx7* and *ckx7 T*. As described earlier, these three single mutants possess shorter fruits than wild type (Figures 1B and 1C, see also Figures 4A and 4B). We focused on active CK forms. However, data for inactive CK forms are presented in Tables 1 and S1.

The active isoprenoid CKs are *c*Z, *t*Z, isopentenyladenine (*IP*), and dihydrozeatin (*DHZ*) (Mok and Mok, 2001; Sakakibara, 2006; Spíchal, 2012). These active bases derive from the direct precursor riboside (R) and riboside monophosphate (RMP) forms (*c*ZR and *c*ZRMP, *t*ZR and *t*ZRMP, *IP*R and *IP*RMP, and *DHZ*R and *DHZ*RMP) (Mok and Mok, 2001; Sakakibara, 2006; Spíchal, 2012). These precursors can be considered active because the CK receptors, which mediate cellular CK response, display sensitivity to these forms (Romanov et al., 2006; Stolz et al., 2011).

At early stages of fruit development, *c*Z-type active bases and precursors increased in all mutants with respect to wild type (Table 1). Notably, the *stk*, *ckx7*, and *ckx7 T* mutants contained more active *c*Z than wild type (Table 1). Moreover, *stk* and *ckx7 T* contained a higher amount of *c*ZR (Table 1). At same stages of silique development, the three single mutants *stk*, *ckx7*, and *ckx7 T* showed a general decrease in active *t*Z (Table 1). In particular, the *stk*, *ckx7*, and *ckx7 T* mutants possessed a low amount of *t*ZR, and a small concentration of *t*ZRMP was measured only in *stk* and *ckx7 T* (Table 1).

More *c*Z-type CKs were present in *ckx7* at late stages. Only the *ckx7* mutant had a higher concentration of the *c*Z base (Table 1). However, the concentration of *c*ZR was higher in the two single *ckx7* mutants than in wild type, and the level of *c*ZRMP in *stk* was lower than in wild type (Table 1). At same developmental stage, *stk* contained more *t*Z-type CKs than wild type (Table 1), and *stk* and *ckx7 T* contained more *t*ZR than wild type at same stages (Table 1). One *t*Z precursor had a different concentration in the two single *ckx7* mutants. A lower quantity of *t*ZRMP was measured in *ckx7* than in wild type, whereas *stk* and *ckx7 T* possessed the same concentration of this precursor as wild type (Table 1).

The concentration of active *IP* in the mutants did not differ from that in wild type at early and late stages of fruit elongation (Table S1). Only the concentration of the precursor *IP*R was lower in *stk* and *ckx7 T* during early stages of fruit elongation, whereas at late stages, *IP*RMP was present at a higher level in *ckx7 T* than in wild type (Table S1). A decrease in the quantity of the *DHZ* precursors

Table 1. Profile of *cZ* and *tZ* CKs in *ckx7*, *ckx7 T*, *stk*, and Col-0

Genotype Stage 13 to 16	Total *cZ* Types	*cZ*	*cZR*	*cZRMP*	*cZOG*	*cZROG*	*cZ7G*	*cZ9G*
Col-0	28.52 ± 3.63	0.40 ± 0.05	3.48 ± 0.21	16.67 ± 3.11	0.31 ± 0.04	2.20 ± 0.18	5.32 ± 0.67	0.14 ± 0.03
ckx7	41.32 ± 3.69**	0.92 ± 0.10***	4.39 ± 0.64	16.62 ± 2.32	0.54 ± 0.07**	2.72 ± 0.39	16.01 ± 1.49***	0.48 ± 0.07***
ckx7 T	43.33 ± 1.68***	0.79 ± 0.08***	4.57 ± 0.68*	20.61 ± 1.34	0.59 ± 0.10**	2.67 ± 0.18*	13.71 ± 0.69***	0.39 ± 0.05***
stk	31.58 ± 04.02	0.54 ± 0.09**	4.54 ± 0.63*	19.74 ± 3.65	0.30 ± 0.02	1.90 ± 0.10*	4.49 ± 0.24	0.08 ± 0.02*
Genotype Stages 13 to 16	Total *tZ* Types	*tZ*	*tZR*	*tZRMP*	*tZOG*	*tZROG*	*tZ7G*	*tZ9G*
Col-0	34.72 ± 3.19	0.45 ± 0.10	10.18 ± 1.15	14.08 ± 1.72	0.98 ± 0.03	0.89 ± 0.06	6.15 ± 0.52	2.00 ± 0.32
ckx7	28.84 ± 2.95	0.44 ± 0.08	7.31 ± 1.15*	10.87 ± 1.64	0.76 ± 0.10**	0.75 ± 0.06*	6.32 ± 0.44	2.39 ± 0.22
ckx7 T	23.89 ± 2.06**	0.33 ± 0.07	6.17 ± 0.96**	7.45 ± 0.73***	0.72 ± 0.06***	0.69 ± 0.13	6.12 ± 0.29	2.41 ± 0.51
stk	27.19 ± 0.92**	0.43 ± 0.07	7.63 ± 1.07*	10.18 ± 1.27*	0.85 ± 0.06*	0.67 ± 0.08**	5.60 ± 0.37	1.83 ± 0.10
Genotype Stages 17-A and 17-B	Total *cZ* Types	*cZ*	*cZR*	*cZRMP*	*cZOG*	*cZROG*	*cZ7G*	*cZ9G*
Col-0	28.36 ± 2.67	0.63 ± 0.10	1.75 ± 0.29	20.49 ± 2.10	0.22 ± 0.02	0.91 ± 0.13	4.18 ± 0.45	0.18 ± 0.02
ckx7	37.20 ± 3.85*	0.91 ± 0.10*	3.38 ± 0.87*	21.37 ± 2.36	0.43 ± 0.07**	1.40 ± 0.14**	9.34 ± 1.06***	0.39 ± 0.05***
ckx7 T	29.52 ± 3.00	0.69 ± 0.03	2.55 ± 0.45*	18.74 ± 2.43	0.30 ± 0.04*	1.19 ± 0.14*	5.38 ± 0.29**	0.23 ± 0.02*
stk	20.71 ± 1.87**	0.52 ± 0.11	1.75 ± 0.33	13.76 ± 1.97**	0.18 ± 0.04	1.06 ± 0.18	3.08 ± 0.19**	0.15 ± 0.01
Genotype Stages 17-A and 17-B	Total *tZ* Types	*tZ*	*tZR*	*tZRMP*	*tZOG*	*tZROG*	*tZ7G*	*tZ9G*
Col-0	43.45 ± 5.55	0.99 ± 0.18	10.59 ± 2.55	24.03 ± 1.72	2.47 ± 0.49	1.73 ± 0.12	2.45 ± 0.13	1.18 ± 0.14
ckx7	19.56 ± 1.54***	0.92 ± 0.20	6.63 ± 1.44	4.07 ± 0.82***	2.12 ± 0.18	1.59 ± 0.09	2.71 ± 0.03*	1.53 ± 0.08*
ckx7 T	53.27 ± 5.95	1.17 ± 0.11	18.94 ± 2.43**	26.04 ± 3.33	1.96 ± 0.21	1.49 ± 0.16	2.48 ± 0.23	1.18 ± 0.21
stk	57.70 ± 3.62**	1.10 ± 0.09	17.27 ± 2.06*	29.16 ± 3.35	3.14 ± 0.28	2.26 ± 0.49	3.23 ± 0.19**	1.54 ± 0.18

The data are in picomoles per gram of fresh weight; means ± SD (n = 4). Total *cis*-Zeatin (total *cZ* types): *cis*-Zeatin (*cZ*), *cis*-Zeatin riboside (*cZR*), *cis*-Zeatin riboside-5′-monophosphate (*cZRMP*), *cis*-Zeatin-O-glucoside (*cZOG*), *cis*-Zeatin riboside-O-glucoside (*cZROG*), *cis*-Zeatin-7-glucosides (*cZ7G*), and *cis*-Zeatin-9-glucoside (*cZ9G*) from stage 13 to stage 16 of fruit development in *ckx7*, *ckx7 T*, *stk*, and Col-0. Total *trans*-Zeatin (total *tZ* types): *trans*-Zeatin (*tZ*), *trans*-Zeatin riboside (*tZR*), *trans*-Zeatin riboside-5′-monophosphate (*tZRMP*), *trans*-Zeatin-O-glucoside (*tZOG*), *trans*-Zeatin riboside-*O*-glucoside (*tZROG*), *trans*-Zeatin-7-glucosides (*tZ7G*), and *trans*-Zeatin-9-glucoside (*tZ9G*) from stage 13 to stage 16 of fruit development in *ckx7*, *ckx7 T*, *stk*, and Col-0. Total *cZ* types: *cZ*, *cZR*, *cZRMP*, *cZOG*, *cZROG*, *cZ7G*, and *cZ9G* at stages 17-A and 17-B of fruit development in *ckx7*, *ckx7 T*, *stk*, and Col-0. Total *tZ* types: *tZ*, *tZR*, *tZRMP*, *tZOG*, *tZROG*, *tZ7G*, and *tZ9G* at stages 17-A and 17-B of fruit development in *ckx7*, *ckx7 T*, *stk*, and Col-0. Statistical analysis was performed using Student's t test (*$p < 0.05$, **$p < 0.01$, ***$p < 0.001$).

DHZR and *DHZ*RMP was observed in the three mutants during early and late stages of fruit growth (Table S1).

In conclusion, similarities were observed in the concentration of active CKs among the three mutants compared with the wild type, which highlights the influence of CKs in determining final fruit size.

STK and *CKX7* Function in the Same Pathway to Regulate Fruit Elongation

Because *CKX7* might function in the same pathway as *STK* to control fruit elongation, we crossed the two single T-DNA mutants *stk* and *ckx7* to create the double *stk ckx7* mutant and measured the length of its fruits. *stk ckx7* possessed shorter siliques than wild type and *ckx7*, but these were not significantly different in length from *stk* siliques (Figures S4A and S4B). To investigate the potential role of CK degradation in the *stk* mutant phenotype, we attempted to complement the *stk* phenotype with the *35S::CKX7* construct. The rationale was that if *stk* is defective in CK degradation because of *CKX7* downregulation, leading to a higher level of CKs in elongating *stk* fruits, *CKX7* overexpression in *stk* might induce the degradation of CKs in fruit tissues and complement the *stk* phenotype. We obtained five independent transformed plants (*stk 35S::CKX7*), and all displayed partial rescue of the *stk* fruit-length phenotype (Figures S4C and S4D). The double-mutant phenotype confirms that STK acts upstream of *CKX7*; however, because *stk* is epistatic to *ckx7* and the overexpression of *CKX7* only partially rescued the *stk* phenotype, *STK* probably regulates fruit elongation via a CK-dependent pathway and a CK-independent pathway (explored later in more detail).

Finally, to corroborate the hypothesis that CKs negatively influence fruit elongation, we exogenously applied 6-benzylaminopurine (BAP) to *stk* and wild-type siliques at stage 13 for 5 days, analyzed the length of the resulting siliques at stage 17-B, and compared it with that of mock-treated control siliques (Figures S4E and S4F). Exogenous BAP treatment resulted in a reduction in fruit length in wild-type siliques when compared with the mock control and a further reduction in the length in *stk* with respect to the mock (Figures S4E and S4F). This confirms that the final fruit length is regulated by CKs.

FUL Is Downregulated in *stk*

To explain the partial rescue of the *stk* short silique phenotype in the transgenic mutant *35S::CKX7*, we investigated alternative pathways required for fruit growth that might be regulated by STK. It has been shown that ARF6 and ARF8 cofunction with FUL to directly activate *MIR172*C expression in the promotion of valve elongation, because miR172c negatively regulates *AP2*, which is a repressor of fruit elongation (José Ripoll et al., 2015). In wild type, the g*FUL:GFP* fusion protein was localized to the valves and the replum upon fertilization at stage 13. However, from stage 14 onward, FUL-GFP expression was reduced (Figures 5A–5E). In *stk*, FUL-GFP expression was lower than in wild type starting from stage 13 and was absent at stages 15 and 16, whereas at stage 17-B, a weak GFP signal was detected in the medial domain of the fruit (Figures 5F–5J). We also confirmed by qPCR that *FUL* is downregulated in *stk* at different fruit developmental stages with respect to wild type (Figure 5K). To study the genetic interaction between the two MADS-box transcription factors STK and FUL, we analyzed the fruit length of the double *stk ful* mutant at stage 17-B (Figures 5L and 5M). *stk ful* displayed shorter fruits than wild type (*stk ful* = 3.79 mm, n = 60; Col-0 = 14.18 mm, n = 60) and both *stk* and *ful* single mutants (*stk* = 8.89 mm, n = 60; *ful* = 4.61 mm, n = 60) (Figures 5L and 5M). The additive phenotype of the double mutant suggests that both MADS-box proteins regulate fruit elongation via two distinct parallel pathways.

Therefore, we compared *MIR172C* and *AP2* expression in *stk* fruits by qPCR with that in wild type. As expected, *MIR172C* expression was lower, whereas *AP2* expression was higher in *stk* with respect to wild type (Figures 5N and 5O). FUL is also necessary to confine *IND* activity within the valve margin (Liljegren et al., 2004). Ectopic lignification caused by increased *IND* expression in the valves of *ful* causes a failure of valve elongation (Liljegren et al., 2004). To confirm that the downregulation of *FUL* in *stk* also affects FUL targets, we analyzed *IND* expression in *stk* fruits at different developmental stages by qPCR and found it to be increased in *stk* compared with wild type (Figure 5P). These data suggest that STK modulates *FUL* expression, which is required to downregulate *AP2* (via miR172c) and *IND*, thereby promoting silique elongation in *Arabidopsis*.

DISCUSSION

STK Is Fundamentally Required for Fruit Growth

The siliques of the *stk* mutant were shorter siliques than those in wild type (Figures 1B and 1C), despite the normal seed set (Mizzotti et al., 2012), demonstrating the importance of this MADS-domain transcription factor in fruit elongation. Activity of the *STK* promoter was observed in the medial domain of the pistils up to stage 13 (Herrera-Ubaldo et al., 2019). We detected STK-GFP protein from fertilization up to stage 16 in the replum and in the valve margin up to stage 17-B, when siliques reach their final size (Figure 1A). It has been reported that genes that are expressed exclusively in the medial domain of the silique can influence the final fruit length. The expression of *REPLUMLESS* (*RPL*) and *NO TRANSMITTING TRACT* (*NTT*) is confined to the medial domain of the fruit, and mutation of either gene results in siliques that are shorter than wild-type siliques (Crawford et al., 2007; Dinneny et al., 2005; Herrera-Ubaldo et al., 2019; Roeder et al., 2003), highlighting the importance of the replum and the ability of genes expressed in this tissue to influence fruit growth.

The Regulatory Interaction of CKs, *STK*, and *CKX7* Is Crucial for Fruit Growth

CKs are centrally important in controlling the cell cycle and cell expansion during the development of roots and pistils (Bartrina et al., 2011; Cucinotta et al., 2016; Street et al., 2016). Different approaches can be used to increase the levels of CKs in plants and thus to study their importance in plant development. One method is to increase the activity of the ISOPENTENYL TRANSFERASE (IPT) enzymes, which synthesize CKs (Sakakibara, 2006), or to inhibit CK degradation by CKX enzymes, which is the approach that we adopted here.

The expression of the synthetic marker line *TCSn::GFP* revealed an increase in CK signaling during the initial stages of fruit growth in *stk* (Figure 2). To better characterize the basis of this increase in CK signaling, we analyzed the expression of various members of the *CKX* family that encode enzymes involved in CK

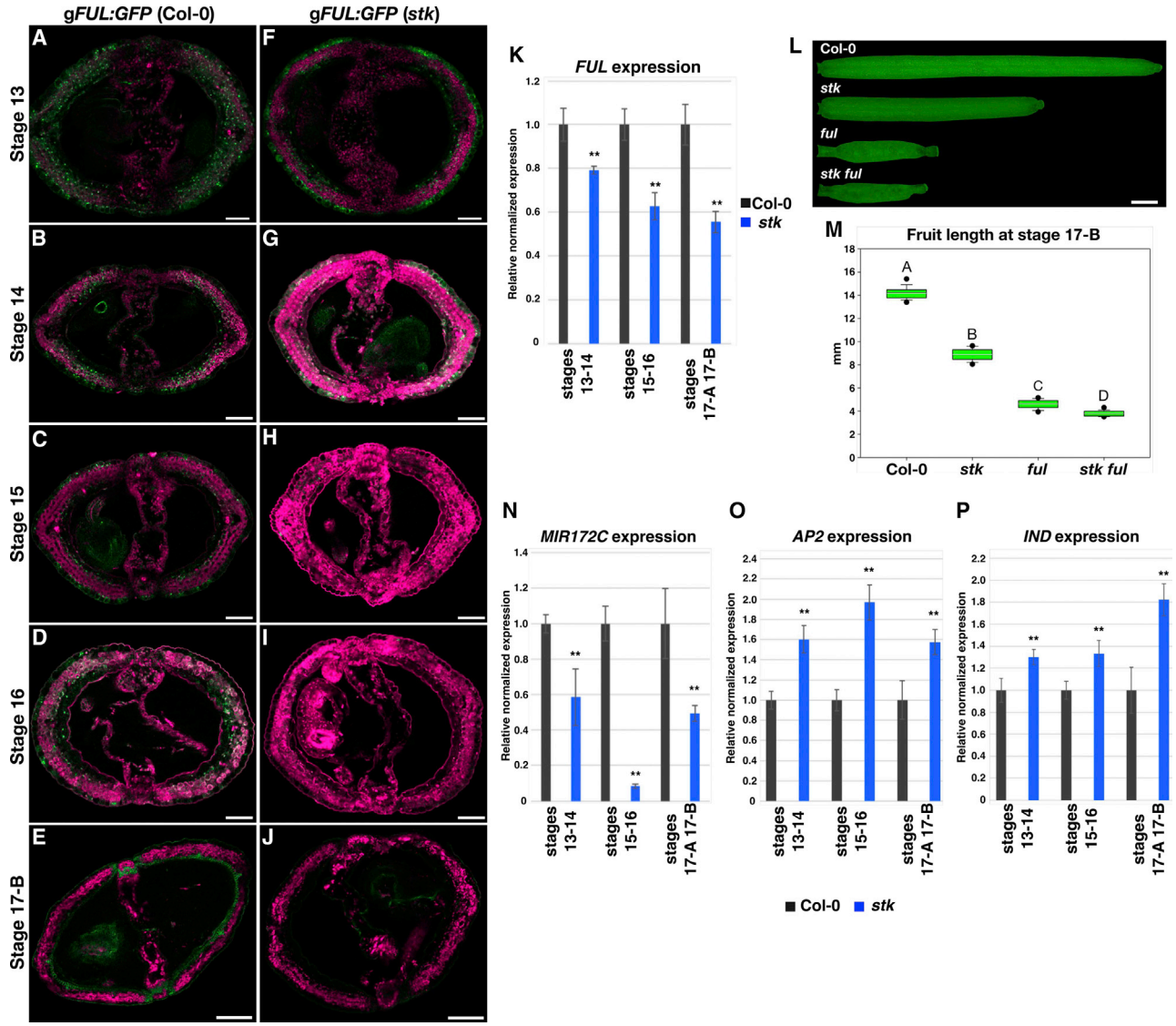

Figure 5. The Role of *STK* in Valve Elongation Pathways

Expression of g*FUL:GFP* in *stk* and Col-0 from stage 13 to stage 17-B.

(A–E) g*FUL:GFP* in Col-0. (A) stage 13 pistil during fertilization, (B) stage 14 of fruit development, (C) stage 15 of fruit development, (D) stage 16 of fruit development, (E) stage 17-B of fruit development. Scale bars, 50 μm.

(F–J) g*FUL:GFP* in *stk*. (F) stage 13 pistil during fertilization, (G) stage 14 of fruit development, (H) stage 15 of fruit development, (I) stage 16 of fruit development, (J) stage 17-B of fruit development. Scale bars, 50 μm.

(K) qPCR to analyze *FUL* expression in *stk* and Col-0 siliques at stages 13–14, 15–16, 17-A, and 17-B. Statistical analysis was performed using Student's t test (**$p < 0.01$). Expression was normalized with *ACTIN* and *UBIQUITIN*. Histograms show a representative experiment in which error bars represent the SD of three technical replicates. Three qPCR (biological replicates) were performed and generated similar results.

(L) Stereomicroscope images of *stk*, *ful*, *stk ful* siliques, and Col-0 at stage 17-B. Scale bar, 1 mm.

(M) Boxplot representing fruit length values of the genotypes described in (L). Boxes indicate the first quartile (Q1), the mean, and the third quartile (Q3); the black dots represent maximum and minimum values. The length of the fruits was evaluated by measuring 20 siliques for each genotype for three biological replicates. Statistical analysis was performed using ANOVA followed by Tukey's HSD test, where different letters indicate statistically significant differences ($p < 0.01$).

(N–P) Expression of (N) *MIR172C*, (O) *AP2*, and (P) *IND* in *stk* and Col-0 siliques at stages 13–14, 15–16, 17-A, and 17-B. Statistical analyses were performed using Student's t test (**$p < 0.01$). Expression data are normalized to expression of *ACTIN* and *UBIQUITIN*. Histograms show a representative experiment in which error bars represent the SD for three technical replicates. Three qPCR (biological replicates) were performed and generated similar results.

degradation (Mok and Mok, 2001; Figure 3A). We found that only *CKX7* was differentially expressed in *stk* and wild type at different fruit developmental stages (Figure 3A). The expressions of *STK* and *CKX7* overlap in the medial domain of the fruit. However, *CKX7* promoter activity was detected not only in the medial domain of the fruit, similar to STK protein (Figure 1A), but also

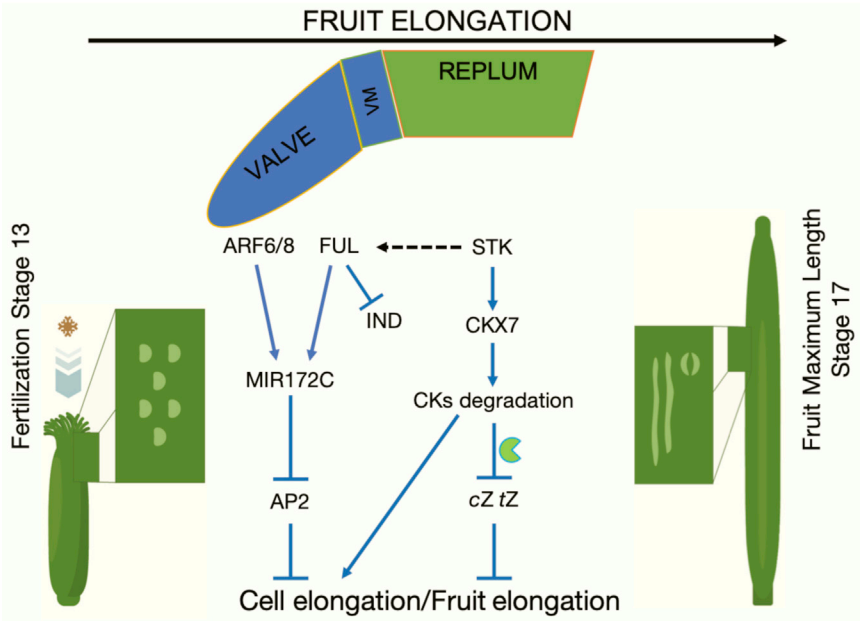

Figure 6. Genetic Model for the Regulation of Fruit Elongation in *Arabidopsis thaliana*

Based on genetic, molecular, and hormonal data presented in this study, we propose a model whereby fruit elongation is regulated by STK, which positively regulates *CKX7* activity in the replum. CKX7 degrades *c*Z and *t*Z CK in fruit cells, leading to an inhibition of cell/fruit elongation. Moreover, STK indirectly regulates *FUL*, which plays a crucial role in the valve elongation pathways. VM, valve margin.

in the lateral vascular bundle of the valves (Figure 3B), in which STK is not expressed. Finally, we demonstrate here that STK is a direct positive regulator of *CKX7* (Figure 3C).

CKX7 Defines Fruit Final Size

We show that the absence of CKX7 activity and the consequent reduction in CK degradation in two *ckx7* mutant alleles caused a dramatic reduction in fruit elongation compared with wild type (Figures 4A and 4B). Conversely, ectopic CK degradation resulting from *CKX7* overexpression in *35S::CKX7* plants resulted in increased fruit length (Figures 4A and 4B). A role for CKX proteins in fruit elongation has been recently suggested based on expression analysis in other closely related species. In particular, an orthologous gene in *Brassica napus*, *BnCKX7-1*, is preferentially expressed in leaves and siliques (Liu et al., 2018; Song et al., 2015). Expression analysis of different *BnCKX* genes from vegetative to reproductive phases revealed that the ortholog of *AtCKX7* is more highly expressed in a *B. napus* cultivar with longer siliques than in one characterized by shorter siliques (Liu et al., 2018). In addition to the results here for *Arabidopsis*, the role of CK in fruit growth appears to be conserved, at least among the Brassicaceae.

Moreover, similar to in the Brassicaceae (Zuñiga-Mayo et al., 2018), exogenous CK treatment in *Arabidopsis* reduces the length of wild-type siliques (Figures S4E and S4F). Treating *stk* with BAP after fertilization causes a further reduction in fruit length (Figures S4E and S4F). The exogenous BAP treatments demonstrate the negative impact of excess CKs on fruit elongation in all Brassicaceae species.

The *stk* and *ckx7* Mutants Have a Higher Amount of CKs during Fruit Growth

The genetic network that regulates CK homeostasis is extremely complex. Therefore, to confirm that the fruit length phenotype described for *stk* and *ckx7* mutants results from an increase in the quantity of CKs, we metabolically profiled the CKs present in fruit mutants with respect to wild type (Tables 1 and S1). At early stages of fruit growth (stages 13 to 16) the endogenous levels of *c*Z bases and the precursors *c*Z and *c*ZR were higher in the mutant than in wild type (Table 1). The amount of *c*Z remained high in the *ckx7* mutant alleles at late stages 17-A and 17-B (Table 1), whereas the concentration of a precursor of the active form (*c*ZRMP) was lower in *stk* than in wild type (Table 1). The lower *CKX7* catalytic activity in *stk* fruits at early stages and the absence of enzymatic activity in the *ckx7* mutant alleles at early and late stages caused an increase in *c*Z forms. This conclusion is consistent with the observation that *c*Z-type CKs are significantly reduced when *CKX7* is overexpressed in seedlings (Köllmer et al., 2014).

By contrast, we detected a general reduction in the concentration of *t*Z bases and their precursor in the mutants compared with wild type at early stages of fruit elongation (Table 1). However, at late stages, *stk* contained a higher amount of *t*Z-type CKs (Table 1), in particular, an increased concentration of *t*ZR, similar to *ckx7 T*. The *t*Z-type CKs are considered a lower-affinity substrate for the CKX7 enzyme (Galuszka et al., 2007; Köllmer et al., 2014; Kowalska et al., 2010). However, at late stages of fruit elongation, we detected a large increase in the amount of *t*Z types not only in *stk* and *ckx7* but also in *ckx7 T* (Table 1). These data suggest that the CKX7 enzyme might have different substrate affinities toward *t*Z at different developmental stages. At late developmental stages, the substrate affinity for CKX7 might be the same as that for *c*Z and *t*Z. In conclusion, the three mutants contained similar concentrations of *c*Z and *t*Z during different stages of fruit development with respect to wild type.

The concentration of active *IP* CKs in the mutants analyzed was relatively similar to that in wild type, whereas the amount of degradation products increased in the *ckx7* mutants throughout fruit growth (Table S1). The data are consistent with those in the literature, because CKX7 has a high affinity for *IP*-type CKs (Galuszka et al., 2007; Köllmer et al., 2014; Kowalska et al., 2010), but further experiments are required to explain the changes in concentration of *IP* CKs in *stk*. During late stages of fruit growth, *stk* contained fewer *IP* degradation products (Table S1).

Finally, the concentration of *DHZ*, a reduced form of *tZ* (Mok and Mok, 2001; Sakakibara, 2006; Spíchal, 2012), was lower in the mutants than in wild type at early and late developmental stages, especially the riboside precursors (*DHZ*R and *DHZ*RMP) (Table S1). These CKs are not degraded by CKXs (Spíchal, 2012). Potentially, the increasing amount of *tZ*, especially at late stages of fruit development, might reduce the concentration of *DHZ* in the mutants compared with the wild type, because this type of CK is a metabolic derivative form of *tZ*.

The Cytosolic CK Pool Must Be Degraded to Promote Cell Elongation in Fruit

In roots, CKs inhibit cell elongation in the primary root by activating typeB ARABIDOPSIS RESPONSE REGULATORs (RESPONSE REGULATORs (ARRs), which in turn, activate the auxin influx carrier AUX1 to modulate auxin transport (Street et al., 2016). The data here suggest that the cytosolic CK pool can potentially repress cell elongation in fruit, similar to in roots. In particular, the cytosolic CK pool, which preferentially consists of *cZ* and *tZ*, might be involved in this repression activity. Notably, CKs have an opposite role in fruit to that in pistils. The importance of CKs in the control of placenta size and number of ovules before fertilization has been demonstrated, and a reduction in the CK transcriptional response in the *crf2 crf3 crf6* triple mutant during pistil development causes a reduction in pistil size and a diminution in total ovule number (Cucinotta et al., 2016). Furthermore, CK signaling mutants show a reduction in pistil size and ovule number (Reyes-Olalde et al., 2017). The positive role of CKs in pistil elongation is confirmed by the *ckx3 ckx5* double mutant, which has longer pistils than wild type because of an increase in CK levels caused by a lack of CKX proteins, with a consequent upregulation of the CK transcriptional response (Bartrina et al., 2011). Before fertilization, CKs promote pistil cell division and elongation and regulate the number of ovule primordia. To facilitate pistil elongation, cell proliferation has to exceed cell differentiation. This is positively regulated by CKs before fertilization and negatively regulated after fertilization.

The Genetic Network Controlled by STK Regulates *FUL* Activity in Fruits

The partial complementation of the *stk* fruit length phenotype by the overexpression of *CKX7* (Figures S4C and S4D) confirms that these two genes act in the same pathway, with STK upstream of CKX7. However, the rescue was only partial, which suggests that STK might act in a pathway independent of that in which *CKX7* expression contributes to the correct degradation of the cytosolic CK pool to appropriately regulate fruit elongation post-fertilization. *FUL* is the most important regulator of valve epidermal cell elongation (Gu et al., 1998). The expression of FUL protein in valves, as monitored via the GFP fusion marker line g*FUL:GFP* (Figures 5A–5J), was lower in *stk* than in wild type. The same result was obtained when we analyzed the transcript levels of *FUL* in *stk* via qPCR (Figure 5K). However, because STK protein is not expressed in valves (Figure 1A), the regulation of *FUL* by STK here is indirect. Similar to in *stk*, *ful* shows increased CK signaling compared with wild type, as monitored by *TCSn::GFP* (Marsch-Martínez et al., 2012). However, increased *TCSn::GFP* expression in *stk* was observed in the replum (Figure 2), which spatially overlapped *STK* expression (Figure 1A), whereas the increased GFP signal in *ful* was present in the valves (Marsch-Martínez et al., 2012) and spatially overlapped *FUL* expression (Figures 5A–5E). The additive phenotype of the double *stk ful* mutant (Figures 5L and 5M) suggests that both MADS-box transcription factors regulate fruit elongation via parallel pathways. The decrease in FUL protein expression in *stk* subsequently downregulates *MIR172* gene expression (Figure 5N), which is essential to promote valve elongation by inhibiting AP2 (José Ripoll et al., 2015), the expression of which is upregulated in *stk* (Figure 5O). Finally, *IND* expression was upregulated in *stk* (Figure 5P). It is known that *IND* expression in *ful* mutant valves causes ectopic lignification and is considered responsible for the lack of cell elongation in *ful* mutant valve cells (Liljegren et al., 2004). These data suggest that STK might influence pathways independent of the *STK-CKX7* pathway described earlier, such as the FUL-MIR172-AP2 and FUL-IND pathways that control valve elongation.

A central unanswered question in plant developmental biology is the identification of hormone-sensing mechanisms and signal transduction pathways that connect regulatory pathways with the activation of developmental programs. Transcriptional networks and hormonal pathways are highly interconnected, and the identification of branchpoints will help to clarify the components that determine the dynamic growth of specific tissues during differentiation. Taking into account the data presented here, we propose a major role for STK in the integration of two pathways, whereby CKs in general and *cZ* and *tZ* levels in particular critically control fruit size (Figure 6).

STAR★METHODS

Detailed methods are provided in the online version of this paper and include the following:

- KEY RESOURCES TABLE
- LEAD CONTACT AND MATERIALS AVAILABILITY
- EXPERIMENTAL MODEL AND SUBJECT DETAILS
  - Plant material and growth conditions
- METHODS DETAILS
  - Binary vector construction and *Arabidopsis* transformation
  - CRISPR Cas9 genome editing to generate ckx7 T
  - Pistil and silique length analysis
  - Scanning electronic microscopy
  - Confocal analysis
  - GUS Assay
  - Expression analysis
  - ChIP assay
  - Hormone treatment
  - Quantification of endogenous cytokinins
  - Feulgen staining for siliques
- QUANTIFICATION AND STATISTICAL ANALYSIS
- DATA AND CODE AVAILABILITY

SUPPLEMENTAL INFORMATION

Supplemental Information can be found online at https://doi.org/10.1016/j.celrep.2020.01.101.

ACKNOWLEDGMENTS

We thank J. Irepan Reyes-Olalde for helpful suggestions on the confocal imaging of *TCSn::GFP* and g*FUL:GFP*. We also thank Charlotte Morgado, Paulo Roberto Llerena Leon, and Domenico Loperfido for help with phenotypic analysis. Part of this work was carried out at NOLIMITS, the advanced imaging facility of the Università degli Studi di Milano. Some experiments were performed in the frame of the H2020-MSCA RISE project (ExpoSeed GA-691109). I.E. acknowledges the Università degli Studi di Milano (Linea 2-DBS), and M.A.M. acknowledges the Foundation for Science and Technology Portugal (FCT-SFRH/BPD/99936/2014). The work was also supported by the Czech Science Foundation (project 18-07563S). Work in the S.d.F. laboratory was also financed by Mexican National Council of Science and Technology (CONACyT) grants CB-2012-177739 and FC-2015-2/1061.

AUTHOR CONTRIBUTIONS

M.D.M. performed most experiments and wrote the manuscript. H.H.-U. performed the GUS assays. E.C. performed scanning electron microscopy (SEM) imaging. O.N. and M.S. performed CK metabolic analysis. V.B. and I.E. helped with the main experiments and writing the manuscript. M.A.M. and S.d.F. designed the experimental strategy and helped to write the manuscript. All authors analyzed the data. L.C. designed the research and wrote the manuscript.

DECLARATION OF INTERESTS

The authors declare no competing interests.

Received: July 1, 2019
Revised: September 13, 2019
Accepted: January 29, 2020
Published: February 25, 2020

REFERENCES

Alabadí, D., Blázquez, M.A., Carbonell, J., Ferrándiz, C., and Pérez-Amador, M.A. (2009). Instructive roles for hormones in plant development. Int. J. Dev. Biol. *53*, 1597–1608.

Bae, E., Bingman, C.A., Bitto, E., Aceti, D.J., and Phillips, G.N., Jr. (2008). Crystal structure of *Arabidopsis thaliana* cytokinin dehydrogenase. Proteins *70*, 303–306.

Bartrina, I., Otto, E., Strnad, M., Werner, T., and Schmülling, T. (2011). Cytokinin regulates the activity of reproductive meristems, flower organ size, ovule formation, and thus seed yield in *Arabidopsis thaliana*. Plant Cell *23*, 69–80.

Braselton, J.P., Wilkinson, M.J., and Clulow, S.A. (1996). Feulgen staining of intact plant tissues for confocal microscopy. Biotech. Histochem. *71*, 84–87.

Clough, S.J., and Bent, A.F. (1998). Floral dip: A simplified method for Agrobacterium-mediated transformation of Arabidopsis thaliana. Plant J. *16*, 735–743.

Crawford, B.C.W., Ditta, G., and Yanofsky, M.F. (2007). The NTT gene is required for transmitting-tract development in carpels of *Arabidopsis thaliana*. Curr. Biol. *17*, 1101–1108.

Cucinotta, M., Manrique, S., Guazzotti, A., Quadrelli, N.E., Mendes, M.A., Benkova, E., and Colombo, L. (2016). Cytokinin response factors integrate auxin and cytokinin pathways for female reproductive organ development. Development *143*, 4419–4424.

Cucinotta, M., Manrique, S., Cuesta, C., Benkova, E., Novak, O., and Colombo, L. (2018). CUP-SHAPED COTYLEDON1 (CUC1) and CUC2 regulate cytokinin homeostasis to determine ovule number in *Arabidopsis*. J. Exp. Bot. *69*, 5169–5176.

de Folter, S., and Angenent, G.C. (2006). trans meets cis in MADS science. Trends Plant Sci. *11*, 224–231.

de Folter, S., Urbanus, S.L., van Zuijlen, L.G.C., Kaufmann, K., and Angenent, G.C. (2007). Tagging of MADS domain proteins for chromatin immunoprecipitation. BMC Plant Biol. *7*, 47.

Dinneny, J.R., Weigel, D., and Yanofsky, M.F. (2005). A genetic framework for fruit patterning in *Arabidopsis thaliana*. Development *132*, 4687–4696.

Egea-Cortines, M., Saedler, H., and Sommer, H. (1999). Ternary complex formation between the MADS-box proteins SQUAMOSA, DEFICIENS and GLOBOSA is involved in the control of floral architecture in Antirrhinum majus. EMBO J. *18*, 5370–5379.

Ezquer, I., Mizzotti, C., Nguema-Ona, E., Gotté, M., Beauzamy, L., Viana, V.E., Dubrulle, N., Costa de Oliveira, A., Caporali, E., Koroney, A.S., et al. (2016). The Developmental Regulator SEEDSTICK Controls Structural and Mechanical Properties of the *Arabidopsis* Seed Coat. Plant Cell *28*, 2478–2492.

Fauser, F., Schiml, S., and Puchta, H. (2014). Both CRISPR/Cas-based nucleases and nickases can be used efficiently for genome engineering in *Arabidopsis thaliana*. Plant J. *79*, 348–359.

Ferrándiz, C., Pelaz, S., and Yanofsky, M.F. (1999). Control of carpel and fruit development in *Arabidopsis*. Annu. Rev. Biochem. *68*, 321–354.

Ferrándiz, C., Gu, Q., Martienssen, R., and Yanofsky, M.F. (2000). Redundant regulation of meristem identity and plant architecture by FRUITFULL, APETALA1 and CAULIFLOWER. Development *127*, 725–734.

Galuszka, P., Popelková, H., Werner, T., Frébortová, J., Pospíšilová, H., Mik, V., Köllmer, I., Schmülling, T., and Frébort, I. (2007). Biochemical characterization of cytokinin oxidases/dehydrogenases from *Arabidopsis thaliana* expressed in *Nicotiana tabacum* L. J. Plant Growth Regul. *26*, 255–267.

Gu, Q., Ferrándiz, C., Yanofsky, M.F., and Martienssen, R. (1998). The FRUITFULL MADS-box gene mediates cell differentiation during *Arabidopsis* fruit development. Development *125*, 1509–1517.

Herrera-Ubaldo, H., Lozano-Sotomayor, P., Ezquer, I., Di Marzo, M., Chávez Montes, R.A., Gómez-Felipe, A., Pablo-Villa, J., Diaz-Ramirez, D., Ballester, P., Ferrándiz, C., et al. (2019). New roles of NO TRANSMITTING TRACT and SEEDSTICK during medial domain development in *Arabidopsis* fruits. Development *146*, dev172395.

José Ripoll, J., Bailey, L.J., Mai, Q.A., Wu, S.L., Hon, C.T., Chapman, E.J., Ditta, G.S., Estelle, M., and Yanofsky, M.F. (2015). microRNA regulation of fruit growth. Nat. Plants *1*, 15036.

Köllmer, I., Novák, O., Strnad, M., Schmülling, T., and Werner, T. (2014). Overexpression of the cytosolic cytokinin oxidase/dehydrogenase (CKX7) from *Arabidopsis* causes specific changes in root growth and xylem differentiation. Plant J. *78*, 359–371.

Kowalska, M., Galuszka, P., Frébortová, J., Šebela, M., Béres, T., Hluska, T., Šmehilová, M., Bilyeu, K.D., and Frébort, I. (2010). Vacuolar and cytosolic cytokinin dehydrogenases of *Arabidopsis thaliana*: heterologous expression, purification and properties. Phytochemistry *71*, 1970–1978.

Liljegren, S.J., Ditta, G.S., Eshed, Y., Savidge, B., Bowman, J.L., and Yanofsky, M.F. (2000). SHATTERPROOF MADS-box genes control seed dispersal in *Arabidopsis*. Nature *404*, 766–770.

Liljegren, S.J., Roeder, A.H.K., Kempin, S.A., Gremski, K., Østergaard, L., Guimil, S., Reyes, D.K., and Yanofsky, M.F. (2004). Control of fruit patterning in *Arabidopsis* by INDEHISCENT. Cell *116*, 843–853.

Liu, H., Ding, Y., Zhou, Y., Jin, W., Xie, K., and Chen, L.L. (2017). CRISPR-P 2.0: An Improved CRISPR-Cas9 Tool for Genome Editing in Plants. Mol. Plant *10*, 530–532.

Liu, P., Zhang, C., Ma, J.Q., Zhang, L.Y., Yang, B., Tang, X.Y., Huang, L., Zhou, X.T., Lu, K., and Li, J.N. (2018). Genome-wide identification and expression profiling of cytokinin oxidase/dehydrogenase (CKX) genes reveal likely roles in pod development and stress responses in oilseed rape (*Brassica napus* L.). Genes (Basel) *9*, 168.

Marsch-Martínez, N., Ramos-Cruz, D., Irepan Reyes-Olalde, J., Lozano-Sotomayor, P., Zúñiga-Mayo, V.M., and de Folter, S. (2012). The role of cytokinin during *Arabidopsis gynoecia* and fruit morphogenesis and patterning. Plant J. *72*, 222–234.

Matias-Hernandez, L., Battaglia, R., Galbiati, F., Rubes, M., Eichenberger, C., Grossniklaus, U., Kater, M.M., and Colombo, L. (2010). *VERDANDI* is a direct target of the MADS domain ovule identity complex and affects embryo sac differentiation in *Arabidopsis*. Plant Cell *22*, 1702–1715.

Mendes, M.A., Guerra, R.F., Castelnovo, B., Silva-Velazquez, Y., Morandini, P., Manrique, S., Baumann, N., Groß-Hardt, R., Dickinson, H., and Colombo, L. (2016). Live and let die: a REM complex promotes fertilization through synergid cell death in *Arabidopsis*. Development *143*, 2780–2790.

Mizzotti, C., Mendes, M.A., Caporali, E., Schnittger, A., Kater, M.M., Battaglia, R., and Colombo, L. (2012). The MADS box genes SEEDSTICK and ARABIDOPSIS Bsister play a maternal role in fertilization and seed development. Plant J. *70*, 409–420.

Mizzotti, C., Ezquer, I., Paolo, D., Rueda-Romero, P., Guerra, R.F., Battaglia, R., Rogachev, I., Aharoni, A., Kater, M.M., Caporali, E., and Colombo, L. (2014). SEEDSTICK is a master regulator of development and metabolism in the *Arabidopsis* seed coat. PLoS Genet. *10*, e1004856.

Mizzotti, C., Rotasperti, L., Moretto, M., Tadini, L., Resentini, F., Galliani, B.M., Galbiati, M., Engelen, K., Pesaresi, P., and Masiero, S. (2018). Time-course transcriptome analysis of *Arabidopsis* siliques discloses genes essential for fruit development and maturation. Plant Physiol. *178*, 1249–1268.

Mok, D.W.S., and Mok, M.C. (2001). CYTOKININ METABOLISM AND ACTION. Annu. Rev. Plant Physiol. Plant Mol. Biol. *52*, 89–118.

Novák, O., Hauserová, E., Amakorová, P., Doležal, K., and Strnad, M. (2008). Cytokinin profiling in plant tissues using ultra-performance liquid chromatography-electrospray tandem mass spectrometry. Phytochemistry *69*, 2214–2224.

Pinyopich, A., Ditta, G.S., Savidge, B., Liljegren, S.J., Baumann, E., Wisman, E., and Yanofsky, M.F. (2003). Assessing the redundancy of MADS-box genes during carpel and ovule development. Nature *424*, 85–88.

Reyes-Olalde, J.I., Marsch-Martínez, N., and de Folter, S. (2015). Imaging early stages of the female reproductive structure of *Arabidopsis* by confocal laser scanning microscopy. Dev. Dyn. *244*, 1286–1290.

Reyes-Olalde, J.I., Zúñiga-Mayo, V.M., Serwatowska, J., Chavez Montes, R.A., Lozano-Sotomayor, P., Herrera-Ubaldo, H., Gonzalez-Aguilera, K.L., Ballester, P., Ripoll, J.J., Ezquer, I., et al. (2017). The bHLH transcription factor SPATULA enables cytokinin signaling, and both activate auxin biosynthesis and transport genes at the medial domain of the gynoecium. PLoS Genet *13*, e1006726.

Roeder, A.H., and Yanofsky, M.F. (2006). Fruit Development in Arabidopsis. Arabidopsis Book *4*, e0075.

Roeder, A.H.K., Ferrándiz, C., and Yanofsky, M.F. (2003). The role of the REPLUMLESS homeodomain protein in patterning the *Arabidopsis* fruit. Curr. Biol. *13*, 1630–1635.

Romanov, G.A., Lomin, S.N., and Schmülling, T. (2006). Biochemical characteristics and ligand-binding properties of *Arabidopsis* cytokinin receptor AHK3 compared to CRE1/AHK4 as revealed by a direct binding assay. J. Exp. Bot. *57*, 4051–4058.

Sakakibara, H. (2006). Cytokinins: activity, biosynthesis, and translocation. Annu. Rev. Plant Biol. *57*, 431–449.

Schindelin, J., Arganda-Carreras, I., Frise, E., Kaynig, V., Longair, M., Pietzsch, T., Preibisch, S., Rueden, C., Saalfeld, S., Schmid, B., et al. (2012). Fiji: an open-source platform for biological-image analysis. Nat. Methods *9*, 676–682.

Schmülling, T., Werner, T., Riefler, M., Krupková, E., and Bartrina y Manns, I. (2003). Structure and function of cytokinin oxidase/dehydrogenase genes of maize, rice, *Arabidopsis* and other species. J. Plant Res. *116*, 241–252.

Song, J., Jiang, L., and Jameson, P.E. (2015). Expression patterns of *Brassica napus* genes implicate IPT, CKX, sucrose transporter, cell wall invertase, and amino acid permease gene family members in leaf, flower, silique, and seed development. J. Exp. Bot. *66*, 5067–5082.

Spíchal, L. (2012). Cytokinins—recent news and views of evolutionally old molecules. Funct. Plant Biol. *39*, 267.

Stolz, A., Riefler, M., Lomin, S.N., Achazi, K., Romanov, G.A., and Schmülling, T. (2011). The specificity of cytokinin signalling in *Arabidopsis thaliana* is mediated by differing ligand affinities and expression profiles of the receptors. Plant J. *67*, 157–168.

Street, I.H., Mathews, D.E., Yamburkenko, M.V., Soroushzadeh, A., John, R.T., Swarup, R., Bennett, M.J., Kieber, J.J., and Schaller, G.E. (2016). Cytokinin acts through the auxin influx carrier AUX1 to regulate cell elongation in the root. Development *143*, 3982–3993.

Svačinová, J., Novák, O., Plačková, L., Lenobel, R., Holík, J., Strnad, M., and Doležal, K. (2012). A new approach for cytokinin isolation from *Arabidopsis* tissues using miniaturized purification: pipette tip solid-phase extraction. Plant Methods *8*, 17.

Tan, M., Li, G., Qi, S., Liu, X., Chen, X., Ma, J., Zhang, D., and Han, M. (2018). Identification and expression analysis of the IPT and CKX gene families during axillary bud outgrowth in apple (Malus domestica Borkh.). Gene *651*, 106–117.

Verwoerd, T.C., Dekker, B.M., and Hoekema, A. (1989). A small-scale procedure for the rapid isolation of plant RNAs. Nucleic Acids Res. *17*, 2362.

Vivian-Smith, A., Luo, M., Chaudhury, A., and Koltunow, A. (2001). Fruit development is actively restricted in the absence of fertilization in *Arabidopsis*. Development *128*, 2321–2331.

Werner, T., Motyka, V., Laucou, V., Smets, R., Van Onckelen, H., and Schmülling, T. (2003). Cytokinin-deficient transgenic *Arabidopsis* plants show multiple developmental alterations indicating opposite functions of cytokinins in the regulation of shoot and root meristem activity. Plant Cell *15*, 2532–2550.

Zuñiga-Mayo, V.M., Baños-Bayardo, C.R., Díaz-Ramírez, D., Marsch-Martínez, N., and de Folter, S. (2018). Conserved and novel responses to cytokinin treatments during flower and fruit development in *Brassica napus* and *Arabidopsis thaliana*. Sci. Rep. *8*, 6836.

Zürcher, E., Tavor-Deslex, D., Lituiev, D., Enkerli, K., Tarr, P.T., and Müller, B. (2013). A robust and sensitive synthetic sensor to monitor the transcriptional output of the cytokinin signaling network in planta. Plant Physiol. *161*, 1066–1075.

STAR★METHODS

KEY RESOURCES TABLE

REAGENT or RESOURCE	SOURCE	IDENTIFIER
Antibodies		
anti-GFP polyclonal antibody	Clontech	CAT# 632460; RRID: AB_2314544
Chemicals, Peptides, and Recombinant Proteins		
6-benzylaminopurine (BAP)	Sigma Aldrich	CAT# B3408
Isotope-labeled internal standards	(Novák et al., 2008)	N/A
Experimental Models: Organisms/Strains		
Arabidopsis: *stk-2*	(Pinyopich et al., 2003)	N/A
Arabidopsis: *ckx7*	NASC	SAIL_515_A07
Arabidopsis: *ful-2*	(Ferrándiz et al., 2000)	N/A
Arabidopsis: *stk ckx7*	This study	N/A
Arabidopsis: *stk ful*	This study	N/A
Arabidopsis: *STK::STK-GFP*	(Mizzotti et al., 2014)	N/A
Arabidopsis: *TCSn::GFP*	(Zürcher et al., 2013)	N/A
Arabidopsis: g*FUL:GFP*	(de Folter et al., 2007)	N/A
Arabidopsis: *stk TCSn::GFP*	This study	N/A
Arabidopsis: stk g*FUL:GFP*	This study	N/A
Arabidopsis: *pCKX7::GUS*	(Mendes et al., 2016)	N/A
Arabidopsis: *stk pCKX7::GUS*	This study	N/A
Oligonucleotides		
Fw *ACTIN2/7* (ChIP experiments) CCAATCGTGAGAAAATGACTCAG	(Matias-Hernandez et al., 2010)	AtP_0329
Rev *ACTIN2/7* (ChIP experiments) CCAAACGCAGAATAGCATGTGG	(Matias-Hernandez et al., 2010)	AtP_0330
Fw *PMEI6* CARG-4 (ChIP experiments) TCTCTCTCGATCTCCATTTG	(Ezquer et al., 2016)	RT 1925
Rev *PMEI6* CARG-4 (ChIP experiments) AGAGTAAACGTGATAGGAGA	(Ezquer et al., 2016)	RT 1926
Fw p*CKX7* CARG-4 and 5 (ChIP experiments) AGACAAACGTTAAACCTAAC	This study	Atp_6961
Rev p*CKX7* CARG-4 and 5 (ChIP experiments) TGTACTGAGACATTCGTAG	This study	Atp_6962
Primers for plant genotyping, CRISPR-mediated mutagenesis, and gene expression analyses are listed in Table S2	This study	N/A
Software and Algorithms		
CRISPR-P 2.0	(Liu et al., 2017)	N/A

LEAD CONTACT AND MATERIALS AVAILABILITY

Further information and requests for resources and reagents should be directed to the Lead Contact, Lucia Colombo (lucia.colombo@unimi.it). Plant lines generated in this study will be made available on request, but we may require a completed Materials Transfer Agreement if there is potential for commercial application.

EXPERIMENTAL MODEL AND SUBJECT DETAILS

Plant material and growth conditions

Seeds of *Arabidopsis thaliana* plants were germinated on soil in long-day conditions (16 h light, 8 h dark) at 22°C. All genotypes used in this study were in Columbia-0 (Col-0) ecotype. The *stk*-2 mutant was provided by M. Yanofsky (Pinyopich et al., 2003). The T-DNA insertion mutant for *ckx7* was obtained from the Nottingham *Arabidopsis* Stock Centre (NASC) and was SAIL_515_A07 line (http://arabidopsis.info; see Figure S2B for knockout validation). The *ful-2* mutant was provided by C. Ferrándiz (Ferrándiz et al., 2000). The *stk ckx7* (*ckx7* SAIL_515_A07 allele) and *stk ful* plants were obtained by crossing the single mutants. The *STK::STK-GFP* marker-line used in this work was described in Mizzotti et al. (2014). The transgenic line *TCSn::GFP* was provided by B. Muller (Zürcher et al., 2013). The transgenic line g*FUL:GFP* was provided by S. de Folter (de Folter et al., 2007). The *stk TCSn::GFP* and *stk* g*FUL:GFP* plants were obtained by crossing. The transgenic line *pCKX7::GUS* was provided by N. Baumann and

R. Groß-Hardt (Mendes et al., 2016). The *stk pCKX7::GUS* plants were obtained by crossing. Primers used for genotyping are listed in Table S2.

METHODS DETAILS

Binary vector construction and *Arabidopsis* transformation

For ectopic *CKX7* expression in wild-type and *stk* plants, the *CKX7* cDNA was cloned under the control of the cauliflower mosaic virus (CaMV) *35S* promoter (NOB 2252). The *CKX7* cDNA was amplified by PCR by high-fidelity Phusion DNA polymerase (Thermo Fisher Scientific) using primers Atp_4677 and Atp_4678. The PCR product was then recombined into the pDONR207 vector (BP Gateway reaction) and sequenced. The PCR product cloned into the DONR vector was then recombined into the pB2GW7 binary vector under control of the CaMV *35S* promoter (LR Gateway reaction) according to the manufacturer's instructions (Thermo Fisher Scientific). Positive colonies (NOB 2252) were selected on LB agar plates containing spectinomycin (100 mg/L) and sequenced. Binary vectors were used to transform *Agrobacterium tumefaciens* (NOB 2329) and *Arabidopsis* plants were transformed using the floral dip method (Clough and Bent, 1998). Primers used for cloning and genotyping are listed in Table S2. See Figure S2C for overexpression validation.

CRISPR Cas9 genome editing to generate ckx7 T

The cloning of the construct to generate another *ckx7* mutant allele was performed following the protocol previously described (Fauser et al., 2014). The protospacer sequence was designated with the aid of CRISPR-P 2.0 software (Liu et al., 2017). The primers used to generate the protospacer are listed in Table S2 (Atp_6702 and Atp_6703). The protospacer was cloned into the pEn-Chimera entry vector, then the gRNA was cloned into the destination vector (pDe-Cas9) using Gateway technology. Positive colonies were selected and used to transform Col-0 plants via *Agrobacterium tumefaciens* using the floral dip method (Clough and Bent, 1998). Finally, we analyzed plants with a single insertion without Cas9 in the T3, T4 and T5 generation to obtain three independent biological replicates.

Pistil and silique length analysis

Pistils at stage 13 (*stk*, *ckx7*, *ckx7 T*, *35S::CKX7*, and Col-0) and siliques at stage 17-B for each genotype (*stk*, *ckx7*, *ckx7 T*, *35S::CKX7*, *stk ckx7*, *stk* x *35S::CKX7*, *ful-2*, *stk ful-2* and Col-0) were collected and images were taken using a stereomicroscope. Pistil and fruit length measurements were obtained using Fiji software (Schindelin et al., 2012). Statistical analyses were performed using the Student t test (*$p < 0.05$, **$p < 0.0$) and ANOVA followed by the Tukey's HSD test (*$p < 0.05$, **$p < 0.01$). Each experiment was performed three times.

Scanning electronic microscopy

Biological samples were collected and fixed overnight at 4°C in FAE solution (10 mL formaldehyde 37%, 50 mL absolute ethanol, 5 mL glacial acetic acid and 35 mL deionized water). Fixed tissues were washed with water and post-fixed with aqueous 2% osmium tetroxide for 2 h at room temperature. Tissues were rinsed several times in deionised water and dehydrated in a graded series of ethanol for 15 min per rinse. This step was followed by critical point drying with liquid CO_2 and sputter-coating with gold in a Nanotech sputter coater. Specimens were analyzed using a LEO 1430 Scanning Electron Microscope.

Confocal analysis

Pistils and siliques of *STK::STK-GFP* plants were collected and mounted in water and observed with a Nikon A1 laser scanning confocal microscope. Analysis of *TCSn::GFP* and g*FUL:GFP* was performed using the protocol described by Reyes-Olalde et al. (2015) and confocal fluorescence images were captured using a confocal laser scanning inverted microscope LSM 510 META (Carl Zeiss, Germany).

GUS Assay

Staining for GUS in *stk* and Col-0 backgrounds containing *pCKX7::GUS* was performed as previously described (Herrera-Ubaldo et al., 2019).

Expression analysis

For transcript quantification, total RNA was extracted from siliques at stages 13–14, 15–16, 17-A and 17-B for expression analysis using the LiCl protocol (Verwoerd et al., 1989). For knockout and overexpression validation, RNA was extracted from stages 13 to 16 using the LiCl protocol (Verwoerd et al., 1989). The cDNA was obtained using an IMProm-II™ Reverse Transcription System (Promega). The q-PCR assay was conducted in triplicate in a Bio-Rad iCycler iQ Optical System using the iTaq Universal SYBR Green Supermix, Bio-Rad (Bio-Rad, http://www.bio-rad.com). The relative transcript enrichment of genes of interest was calculated by normalizing against two housekeeping genes (*ACTIN* and *UBIQUITIN*). Statistical differences were identified with the Student t test (**$p < 0.01$). The primers used for qPCR are listed Table S2.

ChIP assay

The *CKX7* promoter region was analyzed to identify potential CArG boxes. The ChIP experiment was performed as previously described in Ezquer et al. (2016). One gram of silique material from stages 14 to 16 was used for chromatin extraction from *STK::STK–GFP* (Mizzotti et al., 2014) and Col-0 wild-type plants. For immunoprecipitation, we used 1.5 μL anti-GFP polyclonal antibody for each sample (Clontech 632460). Enrichment of the target regions was calculated by qPCR (iTaq Universal SYBR Green Supermix, Bio-Rad) using a Bio-Rad iCycler iQ optical system. The relative enrichment of the targets obtained from *STK::STK–GFP* siliques was compared with the enrichment obtained from wild type. *ACTIN* 2/7 was used for normalization as previously described (Matias-Hernandez et al., 2010). To establish the efficiency of the chromatin immunoprecipitation, we used the fourth CArG box of *PMEI6* as a positive control (Ezquer et al., 2016). Three independent ChIP experiments were performed. The primers used are listed in the Key Resources Table and Table S2.

Hormone treatment

Seeds of *stk* and Col-0 were germinated in a growth chamber, and plants were grown in soil under standard greenhouse conditions. Two weeks after bolting, Col-0 and *stk* plants were treated with a drop application on the pistil at stage 13 (anthesis) and subsequent siliques were treated for 5 days with 100 μM 6-benzylaminopurine (BAP, SigmaAldrich, https://www.sigmaaldrich.com) 0.02% Silwet L-77 (SigmaAldrich) or a mock solution (0.02% Silwet L-77 in NaOH 1M). Silique length was measured one week after the end of the treatment. Statistical analysis was performed using ANOVA followed by Tukey's HSD test (**$p < 0.01$).

Quantification of endogenous cytokinins

Quantification of CK metabolites was performed as previously described in Svačinová et al. (2012). Approximately 0.2 g silique material from stages 14 to 16 (early fruit growth stages) and 17-A and 17-B were harvested for each genotype. Samples (20 mg FW) were extracted in 1.0 mL modified Bieleski buffer (60% MeOH, 10% HCOOH and 30% H_2O) together with a cocktail of stable isotope-labeled internal standards (0.25 pmol CK bases, ribosides, *N*-glucosides, and 0.5 pmol CK *O*-glucosides and nucleotides were added per sample). The extracts were purified using multi-StageTips (containing C18/SDB-RPSS/Cation-SR layers), the eluates were then evaporated to dryness in a vacuum and stored at −20°C. Cytokinin levels were determined using ultra-high performance liquid chromatography-electrospray tandem mass spectrometry (UHPLC-MS/MS) using stable isotope-labeled internal standards as a reference. Four independent biological replicates were harvested for each genotype. Statistical analysis was performed using the Student's t test (*$p < 0.05$, **$p < 0.01$, ***$p < 0.001$).

Feulgen staining for siliques

The reagents used were as described previously (Braselton et al., 1996) with slight modifications. We used 20 different siliques of each genotype at stage 17-B to measure cell length. The samples were excited with an argon ion laser at 488 nm and emissions were detected between 515 and 600 nm. Image capture was performed using a Nikon A1 laser scanning confocal microscope. Statistical analysis consisted of ANOVA followed by the Tukey's HSD test (*$p < 0.05$, **$p < 0.01$).

QUANTIFICATION AND STATISTICAL ANALYSIS

Information about statistical tests used, sample sizes (*n*), and *p-value*s for each experiment are detailed in the relevant STAR Methods sections.

DATA AND CODE AVAILABILITY

Sequence data from this article can be found in the GenBank/EMBL data libraries under the following accession numbers: *AP2*, At4g36920; *CKX1*, At2g41510; *CKX3*, At5g56970; *CKX5* At1g75450; *CKX6*, At3g63440; *CKX7*, At5g21482; FUL, At5g60910; *IND*, At4g00120; *MIR172C* At3g11435; *STK*, At4g09960.